Estimation of the Barrier to Rotation of Benzene in the $(\eta^6\text{-}C_6H_6)_2Cr$ Crystal via Topological Analysis of the Electron Density Distribution Function

Konstantin A. Lyssenko,*,† Alexander A. Korlyukov,† Denis G. Golovanov,† Sergey Yu. Ketkov,‡ and Mikhail Yu. Antipin†

A. N. Nesmeyanov Institute of Organoelement Compounds, Russian Academy of Sciences, 28 ul. Vavilova, 119991 Moscow, Russian Federation and G. A. Razuvaev Institute of Organometallic Compounds, Russian Academy of Sciences, 49 ul. Tropinina, 603600 Nizhnii Novgorod, Russian Federation

Received: December 26, 2005; In Final Form: March 29, 2006

The high-resolution X-ray diffraction analysis of the electron density distribution and plane-wave density functional theory has been applied to estimate the lattice energy and barrier to rotation of a benzene ring in the crystal of $(\eta^6\text{-}C_6H_6)_2Cr$. Experimental data made it possible to perform analysis of the metal−(π-ligand) bond and estimate the nature and energy of weak H···H and H···C intermolecular interactions in the crystal. Summation of the intermolecular H···H and H···C interaction energies makes it possible to reproduce the experimental sublimation enthalpy value with high accuracy.

Introduction

Recently, we have demonstrated that usage of the high-resolution single-crystal X-ray diffraction (XRD) analysis gives extraordinary opportunity to estimate the contribution of the intermolecular interactions into crystal lattice energy ($E_{lattice}$) directly and only from experimental diffraction data.[1,2] The estimation of the intermolecular contacts energy is based on the topological analysis of the electron density distribution function $\rho(\mathbf{r})$ in crystals within Bader's "Atoms in Molecule" (AIM) theory which makes it possible to distinguish the attractive interactions from all other intermolecular contacts.[3] The energy of the former interactions is estimated using the correlation found between the energy of the contact (E_{cont}) with the value of the potential energy density function $\upsilon(\mathbf{r})$ in the corresponding bond critical point (3,−1).[4] The good agreement between the $E_{lattice}$ value obtained and the experimental values of the sublimation enthalphy ΔH°_{subl} can serve as a validation of the accuracy of this approach.[1] Also, the so-obtained $E_{lattice}$ values are close to the corresponding parameters estimated from the periodic quantum-chemical calculations within the plane-wave density functional theory (PW-DFT).[2] Success of the PW-DFT method for estimation of sublimation energy as well as interatomic H-bond energy has been recently demonstrated for crystals of urea,[5] ammonia,[5] and BH_3NH_3.[6]

For example, it was shown within the experimental and theoretical analysis of the $\rho(\mathbf{r})$ in the crystal of 1-phenyl-*o*-carborane that X−H···H−X (X = C, B) intermolecular contacts correspond to the attractive interactions and play a dominating role in the formation of the crystal structure.[1] According to the experimental data, the total energy of the H···H contacts per independent molecule in the crystal (68.6 kJ mol^{-1}) is close to that obtained by the PW-PBE calculation of the crystal (71.1 kJ mol^{-1}).[1] In the case of [2.2]paracyclophane, the total energy of all H···H and H···C contacts per molecule in the crystal according to XRD (91.8 kJ mol^{-1}),[2] is close to the $E_{lattice}$ obtained by the PW-HCTH/120 calculation (95.96 kJ mol^{-1})[2] and to the experimental value of ΔH°_{subl} (96.2 ± 4.2 kJ mol^{-1}).[7]

It should be noted that, in some cases, for example, in metallocenes and arene complexes of transition metals, the energy of intermolecular interactions can be related to other parameters such as barrier to rotation of the cyclic ligand.[8] In this case, an additional verification of the estimated energy value may be obtained, especially if the barrier to internal rotation of the cyclic ligand in an isolated molecule is merely absent. Therefore, it was intriguing to test the validity of the experimental analysis of the electron density function for estimation rotation barrier of the cyclic ligands in classic representative of arene complexes, namely, bis(η^6-benzene)chromium (Bz_2Cr).

The application of the AIM theory for analysis of the nature of the metal−(π-ligand) chemical bonding in metallocenes is rather rare and is limited by topological analysis of the $\rho(\mathbf{r})$ for a series of neutral $M(\eta^5\text{-}C_5H_5)_2$ (M = V, Cr, Mn, Fe, Co, and Ni) 3d-metal complexes within the DFT calculations.[9] This investigation has revealed that the chemical bonding pattern in Fe, Ni, V, and Mn complexes corresponds to the η^5-type coordination of the C_5H_5 ligand while Co and Cr complexes are characterized by the η^1,η^2, and η^3-type coordination, due to Jahn−Teller distortions (see ref 10 and the references therein). It was found in addition that topological parameters of the electron density distribution in the critical points (3,−1) of the M−C bond correlate well with the M−C bond lengths and the value of electron density $\rho(\mathbf{r})$ as well as the energy density function $h_e(\mathbf{r})$ values can be used for estimation of the metal−(π-ligand) interaction energy.[9] It should be noted that the similar results indicating that a shortened contact between the transition metal and cyclopentadienyl ligand cannot be considered as an unambiguous indication of chemical bonding was also observed in a detailed theoretical study of a titanium complex with cyclopentadienyl and cyclohexadiene ligands.[11]

By now, experimental analysis of the electron density distribution in 3d-metal sandwich complexes has been carried out only for few compounds. Available data are limited by the experimental analysis of the deformation electron density

* To whom correspondence should be addressed. E-mail: kostya@xray.ineos.ac.ru.

† A. N. Nesmeyanov Institute of Organoelement Compounds.

‡ G. A. Razuvaev Institute of Organometallic Compounds.

10.1021/jp057516v CCC: $33.50
Published on Web 05/02/2006

TABLE 1: Details of Data Collection and Refinement of $Cr(\eta^6\text{-}C_6H_6)_2$

	$Cr(\eta^6\text{-}C_6H_6)_2$
M	208.22
T	100 K
A, Å	9.5714(2)
V, Å^3	876.85(3)
Z	4
space group	$Pa\bar{3}$
density, g cm^{-3}	1.577
$F(000)$	432
μ (Mo Kα), cm^{-1}	12.43
diffractometer	Smart 1000 CCD
absorption correction (Mo Kα)	semiempirical from equivalents
scan technique	ω-scan with 0.3° step in ω
θ_{max}	53
number of measured reflctns	39036
number of independent reflctns (R(int))	1731 (0.0315)
number of observed reflctns with $I > 2\sigma(I)$	1220
Conventional Refinement	
wR2	0.0752
R1 calculated against F	0.0295
GOF	1.005
ρ_{max}/ρ_{min}	0.737/−0.454
Multipole Refinement	
number of reflctns with $I > 3\sigma(I)$	833
R1 calculated against F	0.0165
R_w calculated against F	0.0162
GOF	0.732
ρ_{max}/ρ_{min}	0.182/−0.164

function in crystals of $V(\eta^5\text{-}C_5H_5)_2$,[12] $(\eta^5\text{-}C_5H_5)M(\eta^7\text{-}C_7H_7)$ (M = Ti, V, Cr),[13] $(\eta^5\text{-}C_5H_5)Ti(\eta^8\text{-}C_8H_8)$,[13] $(\eta^5\text{-}C_5H_5)V(\eta^6\text{-}C_6H_6)V\text{-}(\eta^6\text{-}C_6H_6)$[14], and ethylene-bis(1-indenyl)zirconium dichloride.[15] Therefore, in addition to the investigation of intermolecular interactions, it would be interesting to check the validity of the experimental $\rho(\mathbf{r})$ function for estimation topological parameters of the $Cr-C_6H_6$ bond in Bz_2Cr.

To accomplish this in the present paper, we performed topological analysis of the electron density in the crystal and isolated molecule of Bz_2Cr using a high-resolution X-ray diffraction study (XRD) at 100 K and DFT calculation (B3PW91/6-311G**). To obtain additional verification of the crystal lattice energy estimated from the XRD experiment, we also performed the plane-wave DFT calculation using the PBE functional.

Experimental Section

All operations with air- and moisture-sensitive $CrBz_2$ were carried out in an inert atmosphere. $CrBz_2$ was synthesized by the Fischer method[16] and purified by subsequent crystallization and vacuum sublimation. Single crystals of $CrBz_2$ suitable for the high-resolution XRD experiment were prepared by slow sublimation of a polycrystalline sample in an evacuated ampule. The absorption correction was applied semiempirically using the Sadabs program.[17] The details of the X-ray data collection and conventional full-matrix anisotropic−isotropic refinement are listed in Table 1. The experimental electron density in the crystal was obtained by the multipole refinement based on the Hansen−Coppens formalism[18] using the XD program[19] package. The static molecular charge density in this model is described as a sum of rigid pseudoatoms[18] at the nuclear positions (R_j), $\rho(r) = \sum_j \rho_j(r - R_j)$.

Each pseudoatom electron density has the form

$$\rho_j(r_j) = P_{core}\rho_{core}(r_j) + \kappa'^3 P_{val}\rho_{val}(\kappa'^3 r_j) + \sum_{l=0}^{l_{max}} \sum_{m=-l}^{m=+1} \kappa''^3 P_{lm} R_l(\kappa'' r_j) d_{lmp}(\theta_j,\phi_j)$$

where $r_j = r - R_j$. Both ρ_{core} and ρ_{val} are derived from wave functions fitted to a realitivistic Dirac−Fock solution[20] and describe the frozen core with fixed population (P_{core}), and spherical valence density with population P_{val} is varied to allow charge transfer between atoms. The κ' variable allows for concentration or expansion of the charge cloud of the pseudoatom. The last term in the expansion expression describes the asphericity of the valence density by a set of deformation functions composed by the spherical harmonics (d_{lmp}) and radial Slater-type functions with expansion−contraction coefficient κ''.

Before the refinement, all of the C−H bond distances were normalized to the ideal value of 1.08 Å. The refinement for $CrBz_2$ was carried out with electroneutrality constraints. The level of the multipole expansion was hexadecopole for the Cr atom, octopole for the carbon atoms, and dipole for the hydrogens. The scattering factors of the hydrogen atoms were calculated from the contracted radial density functions ($k = 1.2$).

The refinement was carried out against F, the multipole occupancies of the carbon and chromium atom were refined with the m and 3 symmetry restrains, respectively, according to ref 21. The results of the multipole refinement are listed in Table 1. Analysis of the deformation electron density, ELF, and topology of $\rho(\mathbf{r})$ was carried out using the WINXPRO program package.[22]

Computational Methods

Ab intio calculations of the $CrBz_2$ molecule were performed with the Gaussian98 program package[23] at the B3PW91 level. Full optimization with the D_{6h} and D_{6d} symmetry of the molecule was carried out using the 6-311G** basis set. The optimization was followed by the evaluation of the harmonic vibration frequencies. As convergence criteria, the extremely tight threshold limits of 2×10^{-6} and 6×10^{-6} au were applied for the maximum force and displacement, respectively. To enhance the B3PW91 calculations accuracy, the pruned (99,590) grid has been used for integration. Topological analysis of the $\rho(\mathbf{r})$ function was performed using the MORPHY 98 program,[24] on the basis of the wave functions obtained from the B3PW91 calculations.

The quantum-chemical calculations of the $CrBz_2$ crystal have been conducted using the CPMD 3.9.1 DFT code.[25] For optimization of atomic positions (started from the experimental crystal structure) in crystal, a simulated annealing technique was used, followed by the BFGS minimization of the total energy. Vanderbuilt ultrasoft pseudopotentials[26] have been applied to account for core electrons while valence electrons were approximated by the plane-wave expansion with a 30 Ry cutoff. Exchange and correlations terms of total energy were described by the PBE functional.[27] Since DFT does not take into account dispersion interactions, calculated unit cell parameters may be systematically overestimated or underestimated up to 5%. Therefore, the experimental values of the unit cell parameters were used in the calculations. Atomic displacements converged better than 1×10^{-4} au as well as energy variations were less than 1×10^{-6} au.

The isolated molecules were simulated utilizing the same theoretical background, basis sets, and convergence criteria by

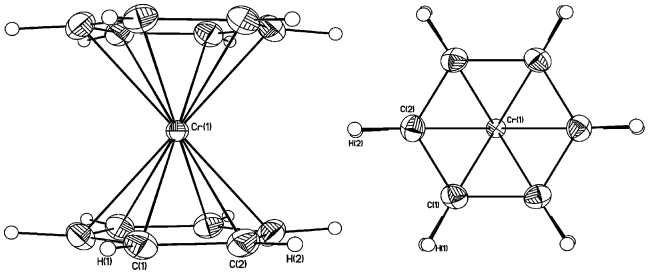

Figure 1. General view of the $CrBz_2$ molecule in two projections with the presentation of atoms by thermal ellipsoids at the 50% probability level.

quantum-chemical calculations of a single molecule in a cubic box with sides of 15 Å. The structures of isolated molecules were tested on stability by calculation of vibrational frequencies, and no negative ones were obtained. Unfortunately, the exact calculation of vibrational frequencies in the case of periodic boundary conditions is difficult for us due to large requirements of computer time. Because of these difficulties, no zero-point correction was applied to the sublimation energy. On the other hand, the plane-wave basis set has no superposition error, in contrast to the ordinary Gaussian basis sets. We believe that the obtained value of sublimation energy can be successfully used as a valuable criterion for characterization of the strength of intermolecular interactions in the crystal.

Results and Discussion

Molecular and Crystal Geometry. The geometry of $CrBz_2$ has been analyzed in details both in the gas phase[28−30] and in the solid state.[29−34] There was a considerable controversy as to whether the molecule in the gas phase possesses a full D_{6h} symmetry, a D_{3d} symmetry with alternating C−C bonds, or a D_{3h} symmetry with alternating C−C bonds (see ref 30 and the references therein). It is accepted now that in the singlet ground state the $CrBz_2$ molecule is characterized by the D_{6h} symmetry.[29]

The crystal of $CrBz_2$ (space group $Pa\bar{3}$, $Z = 4$, $Z' = 0.16$) within the temperature interval 100−325 K,[33] in contrast to 3d-metallocenes $M(\eta^5\text{-}C_5H_5)_2$,[8] does not undergo a phase transition. According to high-resolution XRD, two independent C−C (1.416(1), 1.417(1) Å) and Cr−C (2.1406(6), 2.1409(6) Å) bond lengths are equal (Figure 1). The B3PW91 calculation ideally reproduces the XRD geometry (Table 2). It should be noted that both in the crystal and in the isolated molecule the hydrogen atoms are slightly shifted from the benzene ring plane toward the metal atom.

According to analysis of intermolecular contacts in the crystal of $CrBz_2$, each independent hydrogen atom participates in two contacts assembling neighboring molecules in "trimers" (Figure 2, Table 3). The C−H···H−C contacts for the H(1) and H(2) atoms are slightly different (2.39 and 2.42 Å) and are characterized by the C−H···H angles in the interval 99−151° (Table 3). It should be noted that in the case of the H(2) atom we cannot exclude that these contacts are formed not between the hydrogen atoms but between the hydrogen atom and the benzene π-system. Indeed, the H(2)···C(2′) distance (2.80 Å) and, in particular, C(2)−H(2)···C(2′) angle (151°) indicate that such type of interaction may exist. So, from analysis of the crystal packing, we can suggest that each benzene ligand participates either in twelve H···H contacts or six H···H and six H···C contacts.

An optimized crystal structure of $CrBz_2$ has been obtained also with the PW-PBE calculation. The molecular geometry as well as the contacts mentioned above were found to be close to the experimental values with only a slight decrease in the Cr−C distances (Tables 2−3). To estimate the energy per molecule in the crystal, we carried out an additional calculation deleting all but one molecule from the crystal lattice thus creating a pseudo-isolated molecule (see refs 5 and 6). Taking into account that in both calculations the same basis set and level of theory was used, comparison of the energies for the crystal and isolated molecule gives the energy of the intermolecular interactions that should be close to the sublimation enthalpy. In the case of $CrBz_2$, such a procedure leads to the sublimation energy equal to 66.96 kJ mol^{-1}; this value was found to be close to the available experimental ΔH°_{subl} value (78.2 ± 6.3 kJ mol^{-1}).[35]

Taking into account that intermolecular contacts make the main contribution to the rotation barrier of the two benzene rings in the solid state, we can estimate E_{rot} of a single ring as a half of sublimation energy obtaining finally $E_{rot} = 33.48$ kJ mol^{-1}. The estimation of the E_{rot} value of the benzene ring in the crystal of $CrBz_2$ was a subject of a number of investigations.[33−34,36−37] The potential energy surface for this rotation was investigated by the atom−atom packing energy barrier (AAPEB) calculation,[34,36] proton spin−lattice relaxation time methods (PSLRTMs),[37] and finally, within analysis of atomic anisotropic displacement parameters (ADPs).[33] The barriers obtained within the AAPEB calculation 19.2 and 31.4 kJ mol^{-1} (at room temperature and 78 K, respectively)[34,36] are in agreement with activation energy value (19.1 kJ mol^{-1}) from PSLRTMs.[37] The E_{rot} value from the ADP analysis was obtained for a deuterated $CrBz_2$ sample at nine different temperatures within the interval 100−375 K with a 25 K step.[33] The E_{rot} showed a steady increase from 325 K (25 kJ mol^{-1}) to 175 K where, within the experimental error, a plateau (28.7 kJ mol^{-1}) was attained.[33] Thus, it is apparent from the data presented that the PW-PBE calculation gives a reasonable value for the barrier to rotation in the $CrBz_2$ crystal. To study the nature and energy of the H···H and C···H intermolecular contacts on the basis of the XRD data, we performed topological analysis of the $\rho(\mathbf{r})$ function taken from the X-ray experiment.

Electron Density Distribution. The deformation electron density (DED) maps in the crystal in the benzene ring plane and section passing through the chromium and carbon atoms are characterized by expected features: the uniform distribution of the DED for the benzene ring with insignificant polarization of C−C bond that can be the consequence of crystal packing effects (Figure 3A) and a significant anisotropy of the DED in the vicinity of the metal atom (Figure 3B). In the latter section, two DED maxima near the Cr atom are directed to the ring centers and two other ones are parallel to the benzene rings. The negative DED peaks are located along the Cr−C bond vectors. Similar distribution of the DED around the Cr atom is in line with the results of the 3d-orbital population analysis within the NBO localization scheme (Table 4).

It is known that the chromium configuration in $CrBz_2$ is $(e_{2g})^4(a_{1g})^2(e_{1g})^0$, where MO a_{1g} is nonbonding, e_{2g} is bonding, while e_{1g} is antibonding. The bonding in $CrBz_2$ results from the electron donation from the metal e_{2g} orbital to the corresponding combination of benzene MOs and back-donation from the ligand leads to partial occupation of the chromium e_{1g} orbital. This scheme is illustrated by the NBO analysis (Table 4).

In addition to the NBO scheme, the d-orbital populations is estimated also directly from the multipole population parameters according to ref 38. The values obtained are given in Table 4. Though populations of the a_{1g} and e_{2g} orbitals obtained from the experimental data are systematically lower, the relative populations are quite close to the quantum-chemical data.

TABLE 2: Bond Lengths (angstroms) According to XRD, B3PW91/6-311G, and PW-PBE Calculations and Difference in Energy for D_{6h} and D_{6d} Configurations**

	XRD[a]	PW-PBE	B3PW91/6-311G**	
parameter	D_{6h}	D_{6h}	D_{6h}	D_{6d}
Cr−C	2.1406(6)	2.1195	2.138	2.142
C−C	1.416(1)/1.421	1.421	1.414	1.414
C−H[b]	1.086	1.107	1.086	1.086
Cr−Bz	1.605	1.573	1.604	1.609
δH[c]	0.07	0.074	0.0472	0.0514
E, au			−1508.8459253	−1508.8453310
ZPE, au			0.204660	0.204694
ΔE, kJ mol^{-1}			0	1.64

[a] All values for two independent C(1) and C(2) atoms are averaged. [b] The bond lengths are constrained in accord with the B3PW91/6-311G** calculation. [c] Deviation of the hydrogen atoms from the benzene ring plane toward the Cr atom (angstroms).

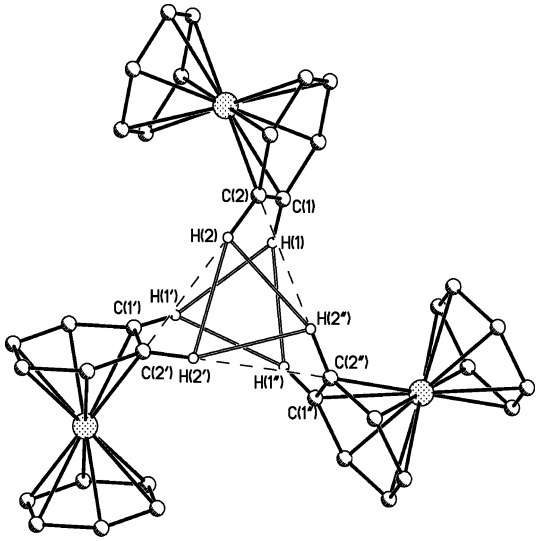

Figure 2. "Trimers" in the crystal of $CrBz_2$. The H···H contacts are shown by open lines, and the H···C contacts are designated by dashed lines.

TABLE 3: Geometrical Parameters of the Probable H···H and C−H···C Contacts in the Crystal of $CrBz_2$

parameter	X-ray	PW-PBE
C(2)−H(2)···C(2′)[a]		
H(1)···H(1′), Å	2.39	2.326
C(1)H(1)H(1′), deg	139	139.2
H(1)H(1′)C(1′) deg	127	129.9
C(2)−H(2)···H(2′)[a]		
H(2)···H(2′), Å	2.42	2.429
C(2)H(2)H(2′), deg	99	97.2
H(2)H(2′)C(2′) deg	151	149.5
C(2)−H(2)···C(2′)[a]		
H(2)···C(2′), Å	2.80	2.793
C(2)−H(2)···C(2′), deg	151	150.4

[a] Atoms with an asterisk are obtained from the basic ones by symmetry operation $0.5 + z$, $0.5 - y$, and $-y$.

In accord with the population analysis, the chromium atomic charge obtained by the integration of the electron density function over the atomic basin (Table 5) is somewhat less than that predicted by the B3PW91/6-311G** calculation. The XRD charge on the chromium atom agrees very well with the NMR data which suggests a transfer of 0.72 e from the metal to the ligands in $CrBz_2$.[39] Negative charges on the C atoms and positive charges on the H atoms estimated in this work on the basis of the XRD experiment and the B3PW91/6-311G** calculation (Table 5) are in accord with the results of numerous other calculations (see ref 30 and the references therein). An additional support for the charges obtained is given by the fact that the independent volume of $CrBz_2$ obtained by summation of the atomic volumes according to the AIM theory (218.87 Å^3) and the experimental one (219.21(3) Å^3) are practically identical.

Topological parameters of the $\rho(\mathbf{r})$ function in $CrBz_2$ in the crystal and isolated molecule are close to each other. At the same time, it should be noted that accuracy of experimental and quantum-chemical $\rho(\mathbf{r})$ functions and/or critical points (CPs) search algorithms used are not sufficient enough and both characteristic sets of CPs do not satisfy the Poincaré−Hopf relationship.[3] The characteristic set for the $CrBz_2$ molecule, in addition to twelve CP(3,−1) for Cr−C bonds, twelve CP(3,−1) for C−C bonds, and twelve CP(3,−1) for C−H bonds, must also include twelve CP(3,+1) for the three-membered CrC_2 rings, two CP(3,+1) for the benzene ring, and finally, two CP(3,+3) for the CrC_6 polyhedrons.

Despite this, the critical point search for the experimental and calculated $\rho(\mathbf{r})$ functions has not revealed the mentioned CP(3,+1) for the benzene ring and the cage CP(3,+3). This discrepancy clearly related to the occupation of the a_{1g} orbital. Indeed, both CP(3,+1) of the benzene ring and CP(3,+3) are located at the 3- or 6-fold axis in the crystal and in the isolated molecule. At the same time, the maxima corresponding to the dz^2 orbital are also observed on the same line which leads to a negligible separation of the (3,+1) and (3,+3) critical points. It should be noted that the same violation of the Poincaré−Hopf relationship was observed in 3d-metallocenes, such as Cp_2-Fe, where the occupation of the a_{1g} orbital also caused the same problem with the CPs location.[9]

Topological characteristics in the CPs (3,−1) in $CrBz_2$ for the experimental and theoretically obtained $\rho(\mathbf{r})$ functions are listed in Table 6. The values of the kinetic energy density $G(\mathbf{r})$ and the electron energy density $H_e(\mathbf{r})$ in CP (3,−1) for the experimental $\rho(\mathbf{r})$ function were evaluated through the semiquantitative approximation proposed by Kirzhnits.[40] According to refs 40 and 41, the $G(\mathbf{r})$ function is described as $(3/10)(3\pi^2)^{2/3}[\rho(\mathbf{r})]^{5/3} + (1/72)|\nabla\rho(\mathbf{r})|^2/\rho(\mathbf{r}) + 1/6\nabla^2\rho(\mathbf{r})]$, which in conjunction with the local virial theorem $(2G(\mathbf{r}) + V(\mathbf{r}) = 1/4\nabla^2\rho(\mathbf{r}))$[3] leads to the expression for potential energy density $V(\mathbf{r})$ and finally to the $H_e(\mathbf{r})$—the sum of potential and kinetic energy densities.

The best agreement between experimental and theoretical data and, in particular, for the $G(\mathbf{r})$ and $H_e(\mathbf{r})$ values in CP (3,−1) is observed for the Cr−C bonds. The variation of the topological parameters for the rest of the bonds may be related in part to the packing effects and, in the case of energy densities, by limitations of the Kirzhnits approximation for covalent bonds.

It can be seen that the C−C and C−H bonds correspond to the shared type of interatomic interactions. In contrast, in the CP (3,−1) of the Cr−C bonds, the Laplacian of the electron density attains a positive value as it was previously observed

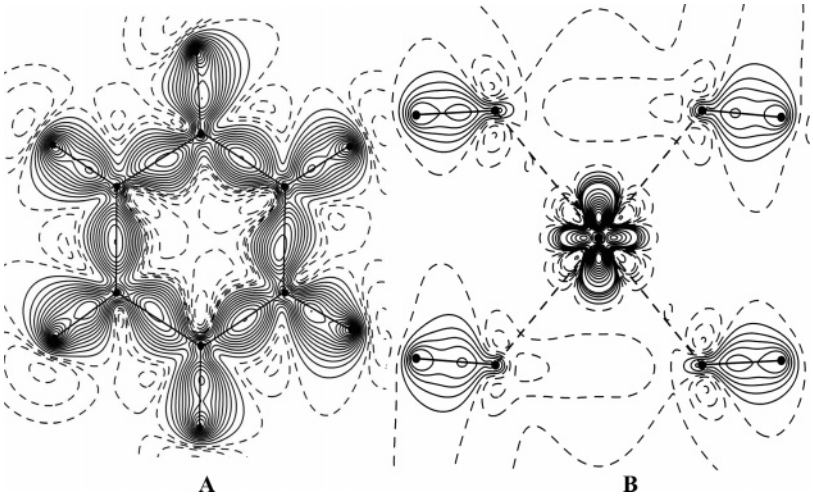

Figure 3. Experimental DED in the plane of the benzene ring (A) and section H(1)C(1)Cr(1) (B) in $CrBz_2$: (A) the contours are drawn through 0.1 e Å^{-3}; (B) the contours are drawn through 0.15 e Å^{-3} for DED values less than 0.3 e Å^{-3} and trough 0.25 e Å^{-3} for the rest. The negative contours are dashed.

TABLE 4: 3d-orbital Populations of the Chromium Atom in $CrBz_2$ According to the NBO Localization Scheme (B3PW91/6-311G) and to the Multipole Refinement of the X-ray Data**

MO	NBO	X-ray
$a_{1g}(d_{z^2})$	1.896/36[a]	1.62(1)/35[a]
$e_{2g}(d_{xy,x^2-y^2})$	2.412/45[a]	1.953(7)/42[a]
$e_{1g}(d_{xz,yz})$	1.026/19[a]	1.112(7)/24[a]

[a] Population in percent.

TABLE 5: Charges of Atoms Obtained by Integration of the Experimental and quantum-chemical $\rho(\mathbf{r})$ Functions over Atomic Basins in the $CrBz_2$

atom	XRD	B3PW91/6-311G**
Cr(1)	0.684	0.941
C(1)	−0.248	−0.142
C(2)	−0.186	−0.142
H(1)	0.164	0.062
H(2)	0.157	0.062

TABLE 6: Topological Characteristics of the $\rho(\mathbf{r})$ in CP (3,−1) in the $CrBz_2$[a]

A−B	$\rho(\mathbf{r})$, e Å^{-3}	$\nabla^2\rho(\mathbf{r})$, e Å^{-5}	ϵ[b]	$G(\mathbf{r})$, a.e.	$H_e(\mathbf{r})$, a.e.
Cr−C	0.484	6.05	7.26	0.0773	−0.0145
	(0.483)	(6.66)	(4.44)	(0.0827)	(−0.0131)
C−C	1.943	−16.83	0.33	0.2439	−0.4185
	(1.971)	(−18.05)	(0.24)	(0.0985)	(−0.2853)
C−H	1.719	−14.10	0.05	0.1972	−0.3423
	(1.865)	(−22.42)	(0.02)	(0.0340)	(−0.2664)

[a] In each column, the upper entry denotes the experimental values and the lower entry in brackets gives a theoretical value from the B3PW91/6-311G** calculations. [b] The ellipticity value.

for various M−X bonds in organometallic compounds (see refs 42 and 43 and the references therein). Although the positive value of the Laplacian is a characteristic of closed-shell interactions, the negative value of $H_e(\mathbf{r})$ clearly indicates that the Cr−C bonds correspond to the intermediate type of interatomic interactions.

It should be noted that application of the Kirzhnits approximation for $G(\mathbf{r})$ not only gives an opportunity to define correctly the type of interatomic interaction but is also a unique way to obtain the electron localization function (ELF)[44] and the localized-orbital locator (LOL)[45] directly from the experimental X-ray diffraction data. Both these functions describe bonding in terms of local kinetic energy density,[46] and in the case of experimentally derived functions, they are preferable for analysis of weak closed-shell interactions.[44,47−48]

Comparison of the experimental and theoretically obtained ELF sections shows that in the vicinity of the chromium atom the ELF distributions are almost identical and close to previously published theoretical data (B3LYP/6-31G*).[49] In contrast, in the area of the C−H bonds, there are some significant distinctions, the main of which is represented by the double peak along the C−H bond (Figure 4). It can be seen also that the Cr···C interactions can be described in terms of peak-hole formalism—the maxima of electron density at carbon atoms are oriented toward the area of the local charge density depletion at chromium. Taking into account that general features of the electron density distribution around the chromium atom as well as the Cr−C interactions are reproduced by the experimental ELF rather well, we conclude that the approximation of ELF proposed by Tsirelson et al.[44] can be used not only for analysis of hydrogen bonds,[44,47] weak dative bonds,[48] and the electron lone pairs domains[47a] but also for description of bonding in various organometallic compounds.

It should be noted that, in addition to the chromium atom, significant anisotropy of ELF distribution is also observed for the hydrogen atoms. Although this effect may be attributed to some discrepancy of ELF in the vicinity of nuclei, it can be also the result of the packing effects.

The critical point search for interatomic contacts in the crystal of $CrBz_2$ has revealed that CPs (3,−1) are located in the area of the H···H contacts (see Table 3, Figure 2). To check that molecules are assembled mostly by H···H intermolecular interactions, and to analyze precisely what type of the contact, H···H or C−H···H, exists in the case of the H(2) atom, we carried out analysis of the bond paths. Indeed, in the case of the H(1) atom, the bond paths starting from CP (3,−1) finish at the hydrogen nucleus (Figure 5A). For the H(2) atom, the situation is different and the bond path links the hydrogen atom with the C(2) one (Figure 5B). Thus, we can conclude that in the crystal of $CrBz_2$ the molecules are assembled by the C(2)−H(2)···C(2′) and C(1)−H(1)···H(1′)−C(1′) interactions while the C(2)−H(2)···H(2′) contact is absent. It should be noted that, in addition to CP (3,−1) in the resulting H···H and H···C connected antiprism (Figure 2), all expected CPs (3,+1) as well as cage CP (3,+3) were found (Figure 5).

Topological parameters of the H···H contacts are close to those in the crystals of 1-phenyl-*o*-carborane[1] and [2.2]paracy-

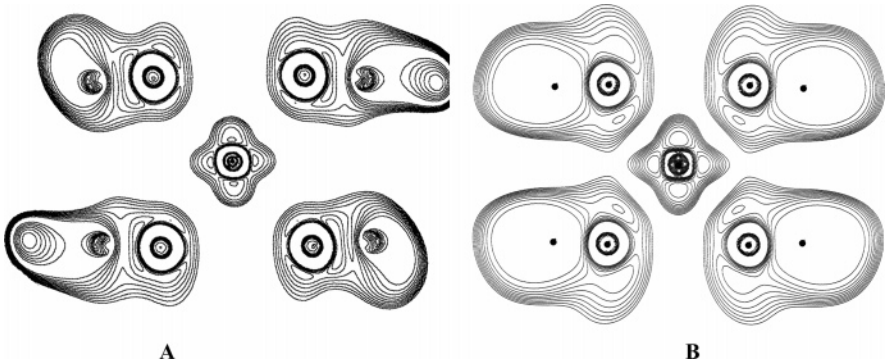

Figure 4. Experimental (A) and theoretically obtained (B) ELF in section H(1)C(1)Cr(1) in $CrBz_2$. The contours with ELF < 0.5 are omitted for clarity.

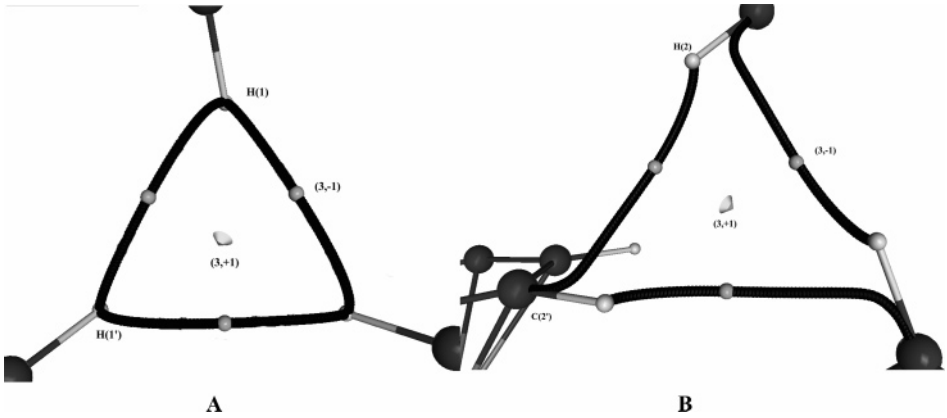

Figure 5. Bond paths for intermolecular contacts in the crystal of $CrBz_2$.

clophane [2] and are comparable with the weak H···H intramolecular interactions recently found in tetra-*tert*-butylcyclobutadiene and tetra-*tert*-butylindacene.[50] In particular, the $\rho(\mathbf{r})$ and $\nabla^2\rho(\mathbf{r})$ values in CPs (3,−1) of the H···H and C···H contacts in the $CrBz_2$ crystal are equal to 0.035, 0.039 e Å^{-3} and 0.35, 0.38 e Å^{-5}, respectively. The corresponding $\rho(\mathbf{r})$ values in the CP (3,+1) and CP (3,+3) formed due to intermolecular contacts in the $CrBz_2$ crystal are equal to 0.023 and 0.017 e Å^{-3}, respectively.

It should be noted that the presence of CPs (3,−1) for the mentioned intermolecular contacts have been observed also for the potential energy density distribution function $V(\mathbf{r})$ (more precisely, $-V(\mathbf{r})$), thus indicating that homeomorphism of the experimental $\rho(\mathbf{r})$ and $-V(\mathbf{r})$ functions (see refs 48 and 51) in the case of weak intermolecular contacts is also satisfied.

The energy of the H···H interactions in the crystal of $CrBz_2$ has been estimated using the correlation proposed by Espinosa et al.[4] Although the energy of the individual interactions is rather small and equal to 2.9 and 3.0 kJ mol^{-1} for the H(1)···H(1′) and H(2′)···C(2′) contacts, respectively, the total energy of interactions for one benzene ligand (six H(1)···H(1′) and six H(2)···C(2′) contacts) will be as high as 35.4 kJ mol^{-1}. Finally, the total energy of all H···H interactions per one molecule of $CrBz_2$ is equal to 70.8 kJ mol^{-1} is close to the corresponding value obtained with the PW/PBE calculation (66.96 kJ mol^{-1}) and to the experimental ΔH°_{subl} value (78.2 ± 6.3 kJ mol^{-1}).[35]

Conclusion

Taking into account that both topological analyses of $\rho(\mathbf{r})$ derived from XRD and the PW-PBE calculation lead to the lattice energy values close to the experimental sublimation enthalpy, and give a good estimation of the barrier to rotation of the benzene ligand in the crystal of $(\eta^6\text{-}C_6H_6)_2Cr$, we may conclude that the energy of the contacts found within the XRD investigation is quite reliable. This work shows that high-resolution XRD investigations of the electron density distribution can not only be used for analysis of the metal−(π-ligand) bond characteristics but also make it possible to reveal and estimate the energy of attractive interactions in the crystal. In the case of the $(\eta^6\text{-}C_6H_6)_2Cr$, this gives an opportunity to estimate the dynamic parameters of the ligand in the crystal assuming the intramolecular barrier is zero. Although in the case of $(\eta^6\text{-}C_6H_6)_2Cr$**,** this method is clearly overcomplicated in comparison with, for example, PW-DFT calculations or analysis of anisotropic displacement parameters, for the crystals containing a number of rigid groups, it has evident advantages providing high-accuracy experimentally based information on nature and energy of intra- and intermolecular interactions in organometallic systems.

Acknowledgment. This work has been supported by the Russian Foundation for Basic Research (Grant Nos. 06-03-32557-a, 03-03-32944) and Support of Leading Schools of the President of the Russian Federation (1153.2006.3, YS-1054.2005.3).

Supporting Information Available: List of atomic parameters in TXT format and CIF information also available. This material is available free of charge via the Internet at http://pubs.acs.org.

References and Notes

(1) Glukhov, I. V.; Lyssenko, K. A.; Korlyukov, A. A.; Antipin, M. Yu. *Russ. Chem. Bull. Int. Ed.* **2005**, *54*, 547.

(2) Lyssenko, K. A.; Korlyukov, A. A.; Antipin, M. Yu. *Mendeleev Commun.* **2005**, 90.

(3) Bader, R. F. W. *Atoms in molecules. A quantum theory*; Clarendron Press: Oxford, U.K., 1990.

(4) (a) Espinosa, E.; Molins, E.; Lecomte, C. *Chem. Phys. Lett.* **1998**, *285*, 170−173. (b) Espinosa, E.; Alkorta, I.; Rozas, I.; Elguero, J.; Molins, E. *Chem. Phys. Lett.* **2001**, *336*, 457−461.

(5) Morrison, C. A.; Siddick, M. M. *Chem.−Eur. J.* **2003**, *9*, 628.

(6) Morrison, C. A.; Siddick, M. M. *Angew. Chem., Int. Ed.* **2004**, *43*, 4780−4782.

(7) (a) Rodgers, D. L.; Westrum, E. F., Jr.; Andrews, J. T. S. *J. Chem. Thermodyn.* **1973**, *5*, 733−739. (b) Boyd, R. H. *Tetrahedron* **1966**, *22*, 119−122.

(8) Braga, D. *Chem. Rev.* **1992**, *92*, 633−665.

(9) Lyssenko, K. A.; Golovanov, D. G.; Antipin, M. Yu. *Mendeleev Commun.* **2003**, 209−211.

(10) Zhen-Feng, X.; Yaoming, X.; Wen-Lin, F.; Shaffer, H. F., III. *J. Phys. Chem. A* **2003**, *107*, 2716−2729.

(11) Bader, R. W. F.; Matta, C. F. *Inorg. Chem.* **2001**, *40*, 5603−5611.

(12) Antipin, M. Yu.; Lyssenko, K. A.; Boese, R. *J. Organomet. Chem.* **1996**, *508*, 259−262.

(13) Lyssenko, K. A.; Antipin, M. Yu.; Ketkov, S. Yu. *Russ. Chem. Bull. Int. Ed.* **2001**, *50*, 130−141.

(14) Angermund, K.; Claus, K. H.; Goddard, R.; Kruger, C. *Angew. Chem., Int. Ed. Engl.* **1985**, *24*, 237.

(15) Stash, A. I.; Tanaka, K.; Shiozawa, K.; Makino, H.; Tsirelson, V. G. *Acta Crystallogr., Sect. B: Struct. Sci.* **2005**, *61*, 418−428.

(16) Fischer, E. O.; Hafner, W. *Z. Naturforsch.* **1955**, *B10*, 665.

(17) Sheldrick, G. M. *SADABS*, Bruker AXS Inc.: Madison, WI, 1997.

(18) Hansen, N. K.; Coppens, P. *Acta Crystallogr. Sect. A: Found. Crystallogr.* **1978**, *34*, 909.

(19) Koritsansky, T. S.; Howard, S. T.; Richter, T.; Macchi, P.; Volkov, A.; Gatti, C.; Mallinson, P. R.; Farrugia, L. J.; Su, Z.; Hansen, N. K. *XD—A Computer program package for multipole refinement and Topological Analysis of charge densities from diffraction data*, 2003.

(20) Su, Z.; Hansen, N. K. *Acta Crystallogr., Sect. A: Found. Crystallogr.* **1998**, *54*, 646.

(21) Jurki-Suonio, K. *Isr. J. Chem.* **1977**, *16*, 115.

(22) (a) Stash, A.; Tsirelson, V. *WinXrpo, A program for Calculation of the Crystal and Molecular properties Using the Model Electron Density*, 2001, further information available at http://xray.nifhi.ru/wxp/. (b) Stash, A.; Tsirelson, V. *J. Appl. Crystallogr.* **2002**, *35*, 371.

(23) Frisch, M. J.; Trucks, G. W.; Schlegel, H. B.; Scuseria, G. E.; Robb, M. A.; Cheeseman, J. R.; Zakrzewski, V. G.; Montgomery, J. A., Jr.; Stratmann, R. E.; Burant, J. C.; Dapprich, S.; Millam, J. M.; Daniels, A. D.; Kudin, K. N.; Strain, M. C.; Farkas, O.; Tomasi, J.; Barone, V.; Cossi, M.; Cammi, R.; Mennucci, B.; Pomelli, C.; Adamo, C.; Clifford, S.; Ochterski, J.; Petersson, G. A.; Ayala, P. Y.; Cui, Q.; Morokuma, K.; Malick, D. K.; Rabuck, A. D.; Raghavachari, K.; Foresman, J. B.; Cioslowski, J.; Ortiz, J. V.; Stefanov, B. B.; Liu, G.; Liashenko, A.; Piskorz, P.; Komaromi, I.; Gomperts, R.; Martin, R. L.; Fox, D. J.; Keith, T.; Al-Laham, M. A.; Peng, C. Y.; Nanayakkara, A.; Gonzalez, C.; Challacombe, M.; Gill, P. M. W.; Johnson, B. G.; Chen, W.; Wong, M. W.; Andres, J. L.; Head-Gordon, M.; Replogle, E. S.; Pople, J. A. *Gaussian 98*, revision A.7; Gaussian, Inc.: Pittsburgh, PA, 1998.

(24) (a) *MORPHY98*, a topological analysis program written by P. L. A Popelier with a contribution from R. G. A. Bone (UMIST, Engl, EU). (b) Popelier, P. *Chem. Phys. Lett.* **1994**, *228*, 160−164.

(25) Hutter, J.; Ballone, P.; Bernasconi, M.; Focher, P.; Fois, E.; Goedecker, S.; Parrinello, M.; Tuckerman, M. *CPMD*, version 3.9.1, 1995−2004, MPI fur Festkorperforschung and IBM Zurich Research Laboratory.

(26) Vanderbilt, D. *Phys. Rev. B: Condens. Matter Mater. Phys.* **1985**, *41*, 7892.

(27) Perdew, J. P.; Burke, S.; Ernzerhof, M. *Phys. Rev. Lett.* **1996**, *77*, 3865.

(28) Haaland, A. *Acta Chem. Scand.* **1965**, *19*, 41.

(29) Rayón, V. M.; Frenking, G. *Organometallics* **2003**, *22*, 3304−3308.

(30) Sahnoun, R.; Mijoule, C. *J. Phys. Chem. A* **2001**, *105*, 6176−6181.

(31) Jellinek, F. *J. Organomet. Chem.* **1963**, *1*, 480.

(32) Keulen, E.; Jellinek, F. *J. Organomet. Chem.* **1966**, *5*, 490.

(33) Jones, R. H.; Doerrer, L. H.; Teat, S. J.; Wilson, C. C. *Chem. Phys. Lett.* **2000**, *319*, 423−426.

(34) Braga, D.; Gepioni, F. *Organometallics* **1991**, *10*, 2563−2569.

(35) Connor, J. A.; Skinner, H. A.; Virmani, Y. *J. Chem. Soc., Faraday Trans. 1* **1973**, *69*, 1218.

(36) Braga, D.; Gepioni, F. *Polyhedron* **1990**, *1*, 53.

(37) Campbell, A. J.; Fyfe, C. A.; Harold-Smith, D.; Jeffrey, K. R. *Mol. Cryst. Liq. Cryst.* **1975**, *36*, 1.

(38) Holladay, A.; Leung, P. C.; Coppens, P. *Acta Crystallogr., Sect. A: Found. Crystallogr.* **1983**, *39*, *377*.

(39) Graves, V.; Lagowski, J. *J. Inorg. Chem.* **1976**, *15*, *577*.

(40) Kirzhnits, D. A. *Sov. Phys. JETP* **1957**, *5*, *64*.

(41) (a) Abramov, Yu. A. *Acta Crystallogr., Sect. A: Found. Crystallogr.* **1997**, *53*, 264. (b) Tsirelson, V. G. *Acta Crystallogr., Sect. B: Struct. Sci.* **2002**, *58*, 632−639.

(42) Pillet, S.; Wu, G.; Kulsomphob, V.; Harvey, B. G.; Ernst, R. D.; Coppens, P. *J. Am. Chem. Soc.* **2003**, *125*, 1937−1949.

(43) Macchi, P.; Sironi, A. *Coord. Chem. Rev.* **2003**, *238−239*, 383−412.

(44) Tsirelson, V.; Stash, A. *Chem. Phys. Lett.* **2002**, *351*, 142.

(45) Tsirelson, V.; Stash, A. *Acta Crystallogr., Sect. B: Struct. Sci.* **2002**, *58*, 780−785.

(46) Savin, A.; Nesper, R.; Wengert, S.; Fassler, T. *Angew Chem., Int. Ed. Engl.* **1997**, *36*, 1809. (b) Schmider, H. L.; Becke, A. D. *J. Mol. Struct. (THEOCHEM)* **2000**, *527*, 51−61.

(47) (a) Lyssenko, K. A.; Grintselev-Knyazev, G. V.; Antipin, M. Yu. *Mendeleev Commun.* **2002**, 128. (b) Lyssenko, K. A.; Lyubetsky, D. G.; Antipin, M. Yu. *Mendeleev Commun.* **2003**, 60.

(48) (a) Lyssenko, K. A.; Antipin, M. Yu.; Gurskii, M. E.; Bubnov, Yu. N.; Karionova, A. L.; Boese, R. *Chem. Phys. Lett.* **2004**, *384*, 40−44. (b) Zhurova, E. A.; Tsirelson, V. G.; Stach, A. I.; Pinkerton, A. A. *J. Am. Chem. Soc.* **2002**, *124*, 4574. (c) Lyssenko, K. A.; Aldoshin, S. M.; Antipin, M. Yu. *Mendeleev Commun.* **2004**, 98−101.

(49) Frison and Sevin. *Internet Electron. J. Mol. Des.* **3**, *222*, 2004.

(50) Matta, C. F.; Hernández-Trujillo, J.; Tang, T.; Bader, R. *Chem.−Eur. J.* **2003**, *9*, 1940−1951.

(51) Bader, R. F. W. *J. Chem. Phys. A* **1998**, *102*, 7314−7323.